Chinese Chemical Letters 36 (2025) 109717

Contents lists available at ScienceDirect

Chinese Chemical Letters

journal homepage: www.elsevier.com/locate/cclet

A novel square-shaped Zr-substituted polyoxotungstate for the efficient catalytic oxidation of sulfide to sulfone

Dongsheng Yang[a], Zixin Li[a], Yaoyao Lian[a], Ziyao Fu[a], Tianjiao Li[a], Pengtao Ma[a,*], Guoping Yang[b,*]

[a] Henan Key Laboratory of Polyoxometalate Chemistry, College of Chemistry and Molecular Sciences, Henan University, Kaifeng 475004, China
[b] School of Chemistry and Materials Science, Jiangxi Key Laboratory for Mass Spectrometry and Instrumentation, East China University of Technology, Nanchang 330013, China

ARTICLE INFO

Article history:
Received 29 January 2024
Revised 26 February 2024
Accepted 1 March 2024
Available online 8 March 2024

Keywords:
Zr-substituted
Square-shaped
Polyoxotungstates
Catalytic oxidation
Sulfide

ABSTRACT

By introduction of hydrogen peroxide into the reaction system of $ZrOCl_2{\cdot}8H_2O$ and $K_{14}[As_2W_{19}O_{67}(H_2O)]$, a novel polyoxometalate $K_8Na_{19.5}H_{0.5}[Zr_2(O_2)_2(\beta\text{-}As^VW_{10}O_{38})]_4{\cdot}68H_2O$ (**1**) has been successfully obtained *via* one-pot method and systematically characterized by IR, XPS, solid UV spectra, PXRD pattern, and TGA analysis. The analysis of X-ray crystallography exhibits that compound **1** crystallizes in the triclinic space group *P*-1 and presents a novel square-shaped Zr-substituted tetrameric polyoxometalate. The catalytic oxidation of sulfides by **1** are carried out, which demonstrate that **1** exhibits a good performance for the catalytic oxidation of sulfides to sulfones with high conversion (100%) and high selectivity (100%).

Polyoxometalates (POMs) are deemed as a crucial class of anion metal-oxo clusters constructed by early transition metals (M = Mo^{VI}, W^{VI}, V^V, Nb^V, and Ta^V), which possess superduper application prospects in medicine, catalysis, optics, magnetism and so on [1–10]. Up to now, the research of POMs has been prevailingly concentrated on lanthanide-substituted and transition-metal-substituted POMs (TMSPs) [11–19]. For lanthanide-substituted lacunary POMs (LSLPs), the reason is that the lanthanide ions (Ln^{3+}) include unfilled 4f orbitals, which can be used for accepting lone pairs of electrons to form covalent bonds from diverse ligands. Hence, the lacunary POMs can be regarded as multi-dentate inorganic ligands to combine with lanthanide ions to obtain more LSLPs. Meanwhile, LSLPs have wide applications in fluorescence, photochromic, catalysis and so on [20,21]. For TMSPs, the introduction of transition metals into the skeleton of POMs can extend the adsorption range from UV to visible light, which is good for their applications in photocatalysis. The majority of the researches of TMSPs are focused on the noble-metal-substituted POMs such as Ru and Rh, and first transition series metal-substituted POMs such as Fe, Co, Ni, Cu, Zn, Ti, Mn [22–27]. Nevertheless, the metal-ions-substituted POMs with high valence like zirconium ion has been less developed. The development of zirconium-substituted POMs (ZrSPs) has been relatively slow probably because that it owns strong oxyphilic character, which makes it easy to bond with the oxygen atoms in the aqueous solution to form precipitate rather than crystallization. Also, the ZrSPs possess wonderful properties in oxygen sensing and catalysis [28]. Therefore, continuously exploring of ZrSPs is of great significance.

Since the first sandwiched-type ZrSP has been reported by Finke *et al.* in 1989 [29], only a small number of ZrSPs have been achieved. In 2005, a sandwiched ZrSP was reported by Hill *et al.*, which was acquired by mixing two chiral tartaric acid or malic acid and $[P_2W_{15}O_{56}]^{12-}$ precursor in conventional aqueous solution [30]. From then on, ZrSPs have reported occasionally. For instance, a dimeric polyanion $[Zr_4O_2(OH)_2(H_2O)_4(\beta\text{-}SiW_{10}O_{37})_2]^{10-}$, and a trimer $[Zr_6O_2(OH)_4(H_2O)_3(\beta\text{-}SiW_{10}O_{37})_3]^{14-}$ were reported by Kortz *et al.* in 2006 [31]. Later, two dimeric polyanions of $[\{P_2W_{15}O_{54}(H_2O)_2\}_2Zr]^{12-}$ and $[\{P_2W_{15}O_{54}(H_2O)_2\}Zr\{P_2W_{17}O_{61}\}]^{14-}$ were gained by Hill's group in 2007 [32]. In 2009, Xue's group also reported a dimer $Na_8K_4[Zr_4O_2(OH)_2(CH_3COO)_2(\alpha\text{-}GeW_{10}O_{37})_2]{\cdot}33H_2O$ [33]. In addition, another sandwiched structure $Cs_6Na_5[Zr_6O_4(OH)_4(H_2O)_2(CH_3COO)_5(AsW_9O_{33})_2]{\cdot}80H_2O$ was obtained by Kortz *et al.* in 2010 [34]. In 2014, Yang's group got a high-nuclearity ZrSP $Na_{10}K_{22}[Zr_{24}O_{22}(OH)_{10}(H_2O)_2(W_2O_{10}H)_2(GeW_9O_{34})_4(GeW_8O_{31})_2]{\cdot}85H_2O$ under hydrothermal conditions [35]. It is the highest number of Zr^{4+} ions implanted into the skeleton of lacunary POMs up to now. Later, they also reported some other novel ZrSPs such as a tetrameric ZrSP $K_2Na_6H_{10}(Hpy)_3[SbZr_7O_6(OH)_4$

* Corresponding authors.
E-mail addresses: mpt@henu.edu.cn (P. Ma), erick@ecut.edu.cn (G. Yang).

https://doi.org/10.1016/j.cclet.2024.109717
1001-8417/

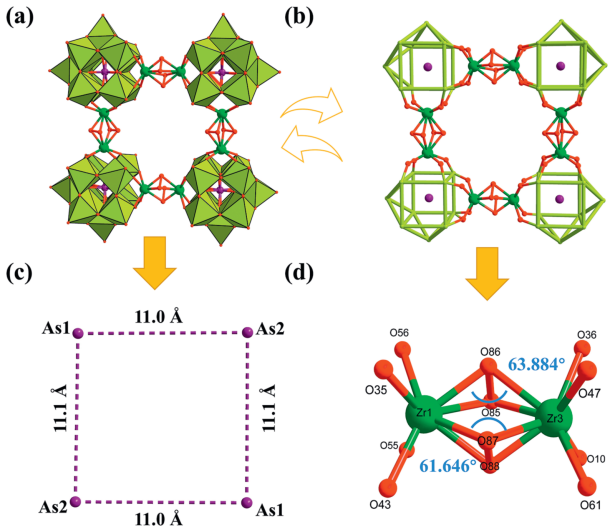

Fig. 1. (a) The ball-and-stick/polyhedral exhibition of **1**. (b) A simplified pattern of **1**. (c) The position and distance of four As atoms in the structure of **1**. (d) The ball and stick exhibition of $\{Zr_2\}$.

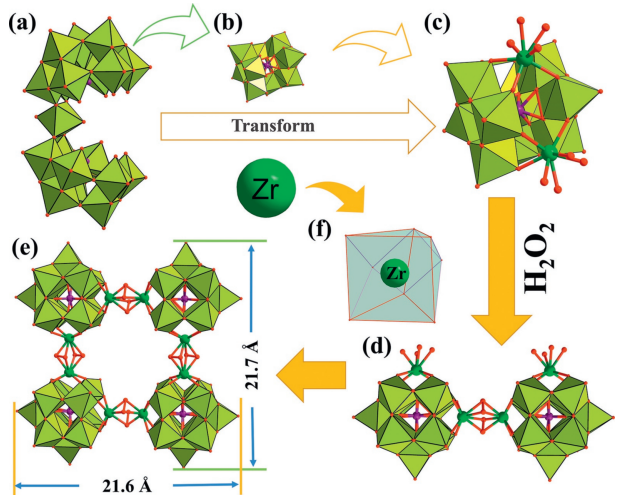

Fig. 2. (a-d) The ball-and-stick/polyhedral exhibition of $[As_2W_{19}O_{67}(H_2O)]^{14-}$, $[\beta\text{-}AsW_{10}O_{38}]^{11-}$, $[Zr_2(\beta\text{-}AsW_{10}O_{38})]^{3-}$ and $[Zr_2(\beta\text{-}AsW_{10}O_{38})]_2^{6-}$, respectively. (e) The size of **1**. (f) The coordination environment of Zr atom in **1**.

$(B\text{-}\alpha\text{-}GeW_9O_{34})_2(B\text{-}\alpha\text{-}GeW_{11}O_{39})_2]\cdot 28H_2O$ and a trimeric ZrSP $[H_2N(CH_3)_2]_{10}H_{14}[(Zr_2P_2W_{16}O_{61})_3]\cdot 7H_2O$ and so on [36–42].

Based on the literature researches, we found the majority of the reported ZrSPs are sandwiched structures. The multimers in ZrSPs were sporadically reported. Herein, we attained a novel tetrameric compound $K_8Na_{19.5}H_{0.5}[Zr_2(O_2)_2(\beta\text{-}As^VW_{10}O_{38})]_4\cdot 68H_2O$ (**1**) utilizing $K_{14}[As_2W_{19}O_{67}(H_2O)]$ as precursor *via* conventional aqueous solution [43]. Considering the introduction of peroxyl bond in the complex, the catalytic oxidation reactions of sulfides with H_2O_2 were implemented. The results demonstrate that **1** exhibits a good performance for the catalytic oxidation of sulfides to sulfones with high conversion (100%) and high selectivity (100%).

Compound **1** is crystallized in the triclinic *P*-1 space group according to the analytic result of single crystal X-ray diffraction data (Table S1 in Supporting information). The result of the power X-ray diffraction pattern is in line with data obtained from the single crystal data, indicating that the high purity of the sample (Fig. S1 in Supporting information).

The symmetric structure of **1** is comprised of a new tetrameric polyanion $[Zr_2(O_2)_2(\beta\text{-}AsW_{10}O_{38})]_4^{28-}$ (**1a**), 8 K^+, 19.5 Na^+, 0.5H^+, and 68 lattice water molecules. **1a** is made up of four divacant $[\beta\text{-}AsW_{10}O_{38}]^{11-}$ $\{AsW_{10}\}$ subunits, and four $[Zr_2(O_2)_2]^{4+}$ $\{Zr_2\}$ fragments. The $[\beta\text{-}AsW_{10}O_{38}]^{11-}$ subunit in **1a** is rare compared with the common polyanion $[\alpha\text{-}AsW_{10}O_{36}]^{9-}$ (Fig. S3 in Supporting information). In the structure of **1a**, the polyanion exhibits an interesting symmetry, whose whole configuration looks like a square (Fig. 1a). The structure of **1a** can be considered as each $\{Zr_2\}$ cation encapsuled by two $\{AsW_{10}\}$ fragments, and the $\{Zr_2\}$ group fills the role of the bridge to connect the four $\{AsW_{10}\}$ subunits to form a fascinating square configuration (Fig. 1b). The distances of four As atoms are almost the same, exhibiting the length of 11.1 Å and 11.0 Å, respectively (Fig. 1c). The $\{Zr_2\}$ group was constituted by two Zr atoms linked by two peroxyl ions, where the peroxyl bonds are in the vital position on enhancing stability of the structure. The dihedral angles of Zr1–O85–O86–Zr3 and Zr1–O87–O88–Zr3 are *ca.* 63.884° and 61.646°, respectively (Fig. 1d). The transformation of $K_{14}[As_2W_{19}O_{67}(H_2O)] \rightarrow \{AsW_{10}\}$ must have happened during the process of reaction (Figs. 2a and b). The structure of **1a** can also be seen as each $\{AsW_{10}\}$ fragment combined with two Zr atoms to form four $[Zr_2(\beta\text{-}AsW_{10}O_{38})]^{3-}$ building units (Fig. 2c), then every two such building units are bridged by two peroxyl bonds (Fig. 2d) *via* Zr–$(O_2)_2$–Zr (Zr1–$(O_2)_2$–Zr3 and Zr2–$(O_2)_2$–Zr4) to form the square-shaped structure $[Zr_2(O_2)_2(\beta\text{-}AsW_{10}O_{38})]_4^{28-}$ with the length about 2.16 nm (Fig. 2e). In **1a**, all the Zr atoms exhibit the same coordination geometry which show an octa-coordinated, two capped triangular prism configurations (Fig. 2f and Fig. S4 in Supporting information). Specifically, each Zr atom is surrounded by four O atoms from the $\{AsW_{10}\}$ building unit and another four O atoms from two peroxyl ions. Bond valence sum (BVS) calculation verified that the valence states of the W, Zr, As atoms were +6, +4, +5, respectively (Table S2 in Supporting information). It is obvious to find that the valence state of the As atoms in the obtained sample is different from the one that comes from the $K_{14}[As_2W_{19}O_{67}(H_2O)]$ precursor, whose valence state of As atom is +3. The introduction of H_2O_2 in the synthetic process plays an important role to obtain the target product. On the one hand, it can act as an oxidant to oxidize As atom in the precursor from +3 to +5, which is verified by XPS spectra (Fig. S2 in Supporting information); on the other hand, it serves as a bridging ligand to link two Zr atoms. Up to date, there are only several hydrogen peroxide functionalized POMs in Zr-substituted POMs [44–46].

This square-shaped ZrSP reminds us of another three square-shaped ZrSPs reported by Yang's group [39], which are obviously different from our square-shaped ZrSP. It is obvious to see that the building block of the compound **1** obtained by us is $[\beta\text{-}As^VW_{10}O_{38}]^{11-}$, while the buliding block of another three compounds obtained by Yang's group is $[\beta\text{-}SiW_{10}O_{38}]^{12-}$. Moreover, the square-shaped compound **1** is linked by peroxyl bonds, while another three compounds obtained by Yang's group are linked by O-bridges or $[BO(OH)_2]^-$ groups.

Organic synthesis plays an important role in the synthesis of high value-added chemicals. The high value-added chemicals such as the oxygenation product (sulfones and sulfoxides) of sulfides possess wide applications in the domain of function materials, synthetic chemistry, biomedicine and so on [47–49]. Therefore, it has attracted more and more researchers to explore a better catalyst to catalyze the oxidation reaction of sulfides under mild conditions. POMs owning their peculiar properties such as high stability, redox properties, are widely accepted as the candidates for catalysis. The catalytic oxidation of sulfides *via* different methods offers a first-hand synthesis strategy for preparing the sulfone. In this research, **1** was chosen as a heterogeneous catalyst to catalyze the sulfides into sulfones in 3 mL acetonitrile solution. The hydrogen peroxide (H_2O_2) was employed as the oxidant for the reaction, because it is regarded as a green oxidant in organic reaction. The methyl

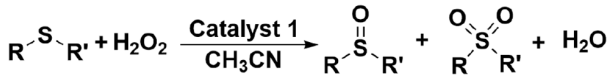

Scheme 1. The catalytic oxidation of sulfides with H_2O_2 catalyzed by **1**.

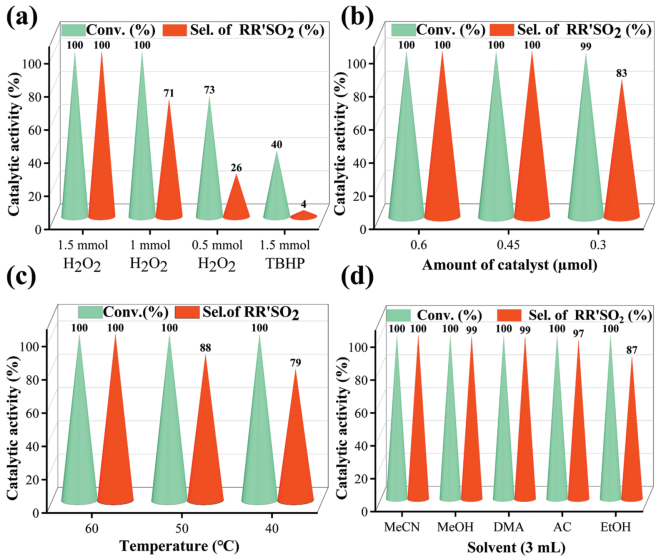

Fig. 3. (a) Impact of the oxidant amount and type of for the catalytic capacity of **1**. (b) Impact of different amount of catalyst on the catalytic capacity of **1**. (c) Impact of the temperature on the catalytic capacity of **1**. (d) Impact of different solvents on the catalytic capacity of **1**. Conditions: MPS (0.5 mmol), catalyst (0.39 μmol), naphthalene (0.39 mmol), solvent (3 mL), 60 °C, and 50 min.

phenyl sulfide (MPS) (0.5 mmol) was employed as the model material and carried out plenty of disparate experiments to investigate the details of the experiments (Scheme 1). The results were decided by gas chromatography-mass spectrometry (GC–MS) and utilized naphthalene as an internal standard to evaluate the conversion of the substrates.

Compound **1** was selected as catalyst to verify the optimum conditions. First of all, the influence of the amount and type of oxidant on the experiment were investigated. When the amount of H_2O_2 is 0.5 mmol, the conversion of MPS is 73% and the selection of $RR'SO_2$ is 26%. The conversion of MPS and selectivity of $RR'SO_2$ increased significantly when the amount of H_2O_2 was added to 1.5 mmol, which changed from 73% and 26% to 100% and 100%. Tert-butyl hydroperoxide (TBHP) was also used as oxidant to the oxidation of sulfides. The results exhibit the conversion of MPS and the selectivity of $RR'SO_2$ is only 40% and 4%, respectively, which is much lower effect than H_2O_2 (Fig. 3a). Additionally, the reaction time also plays an important role in sulfides oxidation reaction. As exhibited in Table S3 (Supporting information), a good conversion of MPS can reach 100%, but a relatively lower yield of $RR'SO_2$ is only 90% during 20 min. when the time was delayed to 50 min, the substrate can totally transform into the target product. The amount of compound **1** was also explored, the results show the best amount of **1** is 0.45 μmol (Fig. 3b). Moreover, the temperature of reaction was also a crucial factor in the process of sulfides oxidation. The substrate can be totally converted but the yield of $RR'SO_2$ is less than 80% in 40 °C. The yield was reached 100% when the temperature of the reaction was increased to 60 °C (Fig. 3c).

In order to verify the universal catalytic effect of **1**, different solvents were selected as reaction medium. As it turned out, the **1** exhibits great catalytic property for oxidation of sulfides in the solvents of acetonitrile (MeCN), methyl alcohol (MeOH), *N*,*N*–diethyl acetamide (DMA), acetone (AC), and ethyl alcohol (EtOH), which demonstrates that the MPS can totally be transformed into $RR'SO_2$

Table 1
The catalytical performance of **1** for MPS oxidation.[a]

Entry	Substrates	Time (min)	Conv. (%)	Sel. of $RR'SO_2$
1		50	100	100
2	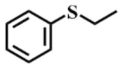	50	100	100
3	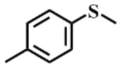	50	100	100
4	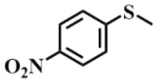	50	100	100
5	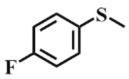	50	100	100
6	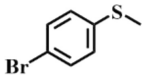	50	100	100
7	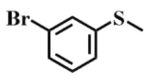	50	100	100
8	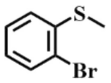	50	98	16
9	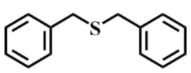	50	99	99
10	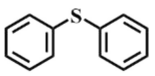	50	99	97

[a] Reaction condition: MPS (0.5 mmol), 30% H_2O_2 (1.5 mmol), catalyst (0.45 μmol), naphthalene (0.39 mmol), MeCN (3 mL), 50 min, and 60 °C.

(Fig. 3d). As a contrast, the blank experiment was also carried out to better verify the catalytic capacity of **1** under same conditions. The results demonstrate that the conversion of the substrate and the yield of the target product was only 35% and 2%. The raw material such as $ZrOCl_2{\cdot}8H_2O$, $K_{14}[As_2W_{19}O_{67}(H_2O)]$ were also employed as catalyst to oxidize MPS (Table S4 in Supporting information). The results demonstrate **1** was a terrific catalyst for the oxidation of MPS. Additionally, the different substrates with electron-withdrawing group or electron-donating groups catalyzed by **1** were investigated. It is easy to find that the conversion of the substrates with disparate groups and yield of the conduct are all quite high (Table 1, entries 1-5). The derivatives of sulfides with groups in different position were also explored. The results verify that the substrate with the group in the “meta-”, “para-”, are easy to be oxidized than that in the “ortho-” position (Table 1, entries 6-8). **1** can be used as catalyst to catalytic most of the substrates included some derivatives with high stereo hindrance (Table 1, entries 9 and 10). Compared with those catalysts summarized in Table S5 (Supporting information), the target compound **1** is superior to the most catalysts with high conversion of sulfides to sulfones (Table S5). The recycling experiments of **1** were carried out. The results demonstrate the excellent yield of $RR'SO_2$ are not decreased obviously after 3 runs (Fig. S6 in Supporting information). Meanwhile, the thermal filtration experiment of **1** was conducted to further verify the heterogeneous nature of this catalyst. **1** was rapidly removed from the reaction mixture by filtration after 5 min and the filtrate continued for another 45 min. The result demonstrated the conversion rate is not significantly improved, indicating the heterogeneity of **1** (Fig. S7 in Supporting information). More-

over, the IR spectrum and PXRD pattern after catalysis was measured and matched well with the fresh one, demonstrating that the catalyst keeps its structure integrity after catalysis (Figs. S8 and S9 in Supporting information).

As shown in Fig. S10 (Supporting information), the reaction mechanism was speculated by us. First, the catalyst reacts with the H_2O_2 to form the electrophilic peroxide intermediates; then the substrate of the sulfides got the O atoms from the electrophilic peroxide intermediates; finally, the electrophilic peroxide intermediates are reduced into the initial conditions for the next recycling. Some similar mechanisms were proposed in the literature formerly [41,50,51].

In conclusion, a novel tetrameric Zr-substituted polyoxotungstate **1**, was successfully obtained by a one-pot reaction. Compound **1** is a tetramer linked by peroxyl bonds. Moreover, the catalytic oxidation of sulfides for **1** has been explored. Notably, compound **1** exhibits prominent performance for the catalytic oxidation of sulfides with high conversion (100%) and high selectivity (100%).

Declaration of competing interest

The authors declare that they have no known competing financial interests or personal relationships that could have appeared to influence the work reported in this paper.

Acknowledgment

This work was financially supported by the National Natural Science Foundation of China (No. 22071043).

Supplementary materials

Supplementary material associated with this article can be found, in the online version, at doi:10.1016/j.cclet.2024.109717.

References

[1] P. Ma, F. Hu, J. Wang, et al., Coord. Chem. Rev. 378 (2019) 281–309.
[2] J.C. Liu, J.F. Wang, Q. Han, et al., Angew. Chem. Int. Ed. 60 (2021) 11153–11157.
[3] Y.F. Liu, C.W. Hu, G.P. Yang, Chin. Chem. Lett. 34 (2023) 108097.
[4] X.D. Liu, N. Xu, X.H. Liu, et al., Chem. Commun. 58 (2022) 12236–12239.
[5] K. Zheng, D. Yang, B. Niu, et al., Inorg. Chem. 61 (2022) 20222–20226.
[6] K. Zheng, P. Ma, Dalton Trans. 53 (2024) 3949–3958.
[7] H. Zhang, W. Zhao, H. Li, et al., Polyoxometalates 1 (2022) 9140011.
[8] J. Li, D. Zhang, Y. Chi, et al., Polyoxometalates 1 (2022) 9140012.
[9] Z.X. Yang, F. Gong, D. Lin, et al., Coord. Chem. Rev. 492 (2023) 215205.
[10] D. Yang, L. Liu, Y. Zhang, et al., Chem. Commun. 60 (2024) 3043–3046.
[11] S.R. Li, W.D. Liu, L.S. Long, et al., Polyoxometalates 2 (2023) 9140022.
[12] B. Yan, R. Liang, K. Zheng, et al., Inorg. Chem. 60 (2021) 8164–8172.
[13] H. Chen, K. Zheng, C. Chen, et al., Inorg. Chem. 61 (2022) 3387–3395.
[14] M. Harris, C. Henoumont, W. Peeters, et al., Dalton Trans. 47 (2018) 10646–10653.
[15] K. Li, Y.F. Liu, X.L. Lin, et al., Inorg. Chem. 61 (2022) 6934–6942.
[16] Y. Liu, L. Li, S. Meng, et al., Inorg. Chem. 62 (2023) 12954–12964.
[17] S.S. Wang, G.Y. Yang, Chem. Rev. 115 (2015) 4893–4962.
[18] S.T. Zheng, G.Y. Yang, Chem. Soc. Rev. 41 (2012) 7623–7646.
[19] J. Liu, N. Jiang, J.M. Lin, et al., Angew. Chem. Int. Ed. (2023) e202304728.
[20] K. Zheng, B. Niu, C. Lin, et al., Chin. Chem. Lett. 34 (2023) 107238.
[21] K. Suzuki, M. Sugawa, Y.J. Kikukawa, et al., Inorg. Chem. 51 (2012) 6953–6961.
[22] H. Li, W. Chen, Z. Yuan, et al., Inorg. Chem. 61 (2022) 9935–9945.
[23] Z. Liu, X. Zhang, R. Wan, et al., Chem. Commun. 57 (2021) 10250–10253.
[24] Q. Hu, S. Chen, T. Wågberg, et al., Angew. Chem. Int. Ed. (2023) e202303290.
[25] J.L. Chen, Z.W. Wang, P.Y. Zhang, et al., Inorg. Chem. 62 (2023) 10291–10297.
[26] L. Schwiedrzik, T. Rajkovic, L. González, ACS Catal. 13 (2023) 3007–3019.
[27] B. Xu, Q. Xu, Q. Wang, et al., Inorg. Chem. 60 (2021) 4792–4799.
[28] C.N. Kato, T. Ogasawara, A. Kondo, et al., Catal. Commun. 96 (2017) 41–45.
[29] R.G. Finke, B. Rapko, T.J.R. Weakley, Inorg. Chem. 28 (1989) 1579–1582.
[30] X. Fang, T.M. Anderson, Y. Hou, et al., Chem. Commun. (2005) 5044–5046.
[31] B.S. Bassil, M.H. Dickman, U. Kortz, Inorg. Chem. 45 (2006) 2394–2396.
[32] X. Fang, C.L. Angew, Chem. Int. Ed. 46 (2007) 3877–3880.
[33] L. Chen, Y. Liu, S. Chen, et al., J Clust. Sci. 20 (2009) 331–340.
[34] G. Al-Kadamany, S.S. Mal, B. Milev, et al., Chem. Eur. J. 16 (2010) 11797–11800.
[35] L. Huang, S.S. Wang, J.W. Zhao, et al., J. Am. Chem. Soc. 136 (2014) 7637–7642.
[36] Z. Zhang, J.W. Zhao, G.Y. Yang, Eur. J. Inorg. Chem. (2017) 3244–3247.
[37] Z. Zhang, B.F. Yang, G.Y. Yang, J. Clust. Sci. 28 (2017) 2565–2573.
[38] Z. Zhang, H.L. Li, Y.L. Wang, et al., Inorg. Chem. 58 (2019) 2372–2378.
[39] H.-L. Li, C. Lian, D.P. Yin, et al., Inorg. Chem. 59 (2020) 12842–12849.
[40] Z. Zhang, Y.L. Wang, Y. Liu, et al., Nanoscale 12 (2020) 18333–18341.
[41] P.Y. Zhang, Y. Wang, L.Y. Yao, et al., Inorg. Chem. 61 (2022) 10410–10416.
[42] H.L. Li, C. Lian, G.Y. Yang, Dalton Trans. 52 (2023) 857–861.
[43] U. Kortz, M.G. Savelieff, B.S. Bassil, et al., Angew. Chem. Int. Ed. 40 (2001) 3384–3386.
[44] B.S. Bassil, S.S. Mal, M.H. Dickman, et al., J. Am. Chem. Soc. 130 (2008) 6696–6697.
[45] S.S. Mal, N.H. Nsouli, M. Carraro, et al., Inorg. Chem. 49 (2010) 7–9.
[46] A. Sundar, N.V. Maksimchuk, I.D. Ivanchikova, et al., Chem. Eur. 2 (2024) e202300066.
[47] M.C. Carreno, Chem. Rev. 95 (1995) 1717–1760.
[48] I.F. Fernandez, N. Khiar, Chem. Rev. 103 (2003) 3651–3705.
[49] M. Han, Y. Niu, R. Wan, et al., Chem. Eur. J. 24 (2018) 11059–11066.
[50] T.Y. Dang, R.H. Li, H.R. Tian, et al., Inorg. Chem. Front. 8 (2021) 4367–4375.
[51] H. Li, C. Lian, L. Chen, et al., Nanoscale 12 (2020) 16091–16101.